Article

*J. Biol. Regul. Homeost. Agents.* 2024; 38(6): 4939–4948
https://doi.org/10.23812/j.biol.regul.homeost.agents.20243806.394

# Exploring the Adaptive Immune Response in Basal Cell Carcinoma: Insights from Efferocytosis-Related Genes

Qiaochu Zhou[1], Wei Wang[2,*]

[1]Department of Dermatology, Wenzhou Hospital of Integrated Traditional Chinese and Western Medicine, 325000 Wenzhou, Zhejiang, China
[2]Department of Gynecology, Wenzhou Hospital of Integrated Traditional Chinese and Western Medicine, 325000 Wenzhou, Zhejiang, China
*Correspondence: w2wangwei@126.com (Wei Wang)
Submitted: 27 January 2023 Revised: 22 February 2023 Accepted: 26 March 2024 Published: 1 June 2024

**Background: The efferocytosis-related genes (EGs) have been associated with the progression of cancers. However, their precise role in basal cell carcinoma (BCC) remains unclear. Therefore, this study aimed to identify biomarkers associated with efferocytosis in BCC.**
**Methods: BCC-related datasets GSE125285 and GSE42109 were extracted. Target genes were identified by intersecting differentially expressed genes (DEGs) identified by "limma". Moreover, the module genes were screened by "weighted gene co-expression network analysis (WGCNA)" and EGs were obtained from the previous literature. Subsequently, the enrichment analysis was conducted employing "ClusterProfiler". Additionally, diagnostic biomarkers for BCC were screened and BCC risk was predicted through a nomogram. Furthermore, an analysis of gene set enrichment analysis (GSEA) was performed to examine possible mechanisms of BCC.**
**Results: A total of 18 target genes were identified by intersecting 7314 DEGs, 6052 module genes, and 71 EGs. These genes were found to be associated with transmembrane transport and phagocytosis. Moreover, five biomarkers (*ADAM10*, *MBTPS1*, *P2RY2*, *SLC2A1*, and *UCP2*) were identified and the diagnostic model was constructed using these biomarkers. Importantly, *MBTPS1* and *P2RY2* were found to be associated with adaptive immune response.**
**Conclusions: This study identified five efferocytosis-related biomarkers that might be used to diagnose BCC. By understanding the regulatory mechanism of EGs in BCC, this study might contribute to further research.**

**Keywords:** basal cell carcinoma; efferocytosis; WGCNA; biomarker

## Introduction

Basal cell carcinoma (BCC) is the most common type of cancer, with a rapidly rising global incidence [1]. There are varying levels of prognosis for BCC, ranging from superficial, nodular lesions that have a good outcome to very extensive, hard-to-treat lesions. Many BCC lesions can be effectively treated through surgical interventions, while those with advanced stages, such as locally advanced and extensive cases, pose significant challenges during treatment [2]. Therefore, there is a need for the development of more effective strategies for early diagnosis and intervention in BCC.

Efferocytosis, which involves the clearance of apoptotic cells by phagocytes, plays a crucial role in suppressing the immune response within tumors [3]. The mechanisms of efferocytosis include the recognition of dying cells, their phagocytic engulfment, and homeostatic resolution. Concretely, efferocytosis elicits an anti-inflammatory response from phagocytes, facilitating tissue repair and maintaining homeostasis. However, abrogation of this process may result in pathophysiological consequences in tumor progression [4–6]. Consequently, we considered that apoptotic and necrotic cells promote tumor progression through efferocytosis. Moreover, a study on osteosarcoma suggested that efferocytosis could be a potential target due to its effects in promoting the expression of PD-L1 and inducing polarization of M2 macrophages [7]. Importantly, the p38/STAT3 pathway has been shown to regulate macrophage phenotypes through efferocytosis mediated by MerTK receptors [3]. Epithelial cancer cells overexpress MerTK receptor tyrosine kinase, resulting in efferocytosis with gain-of-function [8]. Thus, MerTK might be associated with both efferocytosis and cancer progression. Furthermore, the signaling pathways involved in efferocytosis not only play an important role in the growth, invasion, and metastasis of tumor cells but also regulate adaptive responses and resistance to antitumor therapies [9]. These studies strongly demonstrate a significant association between efferocytosis and BCC. However, it is not clear whether efferocytosis-related genes (EGs) contribute as causal factors in BCC pathogenesis.

In this study, we identified five efferocytosis-related biomarkers and constructed a novel diagnostic model for BCC. The findings from this study may provide insights

Journal of
BIOLOGICAL REGULATORS
and Homeostatic Agents

into the identification of potential targets for the diagnosis of BCC, as well as the regulatory mechanisms of EGs in BCC.

## Materials and Methods

### *Data Extraction*

The BCC-related datasets were downloaded from the Gene Expression Omnibus (GEO, https://www.ncbi.nlm.nih.gov/geo/) database. Among them, the GSE125285, including 25 BCC and 25 healthy control (HC) tissue samples, was used as the training dataset to identify the differentially expressed genes (DEGs) and module genes of BCC. However, the GSE42109, comprising 11 BCC and 10 HC tissue samples, was employed as the validation dataset to verify the expression and diagnostic value of predicted biomarkers. Furthermore, a total of 71 EGs were obtained from the previous literature [10,11].

### *Functional Analysis of Target Genes*

Initially, the DEGs between BCC and HC samples identified in the GSE125285 dataset were compared using the "limma" R package (version 3.42.2, Walter and Eliza Hall Institute of Medical Research, Melbourne, Australia) ($|\log_2 FC| > 0.5$, adj.$p$.value $< 0.05$) [12]. After this, the module genes of BCC were screened through the weighted gene co-expression network analysis (WGCNA) employing the "WGCNA" R package (version 1.70.3, University of California, Los Angeles, CA, USA) [13]. Subsequently, the target genes were obtained by intersecting the DEGs, module genes, and EGs using "jvenn". Furthermore, the functional enrichment analysis of these target genes was conducted utilizing the "ClusterProfiler" R package (version 3.14.3, Bioconductor, Guangzhou, China) ($p < 0.05$) [14].

### *Construction of the Diagnostic Model of BCC*

The protein-protein interaction (PPI) network was constructed to investigate the relationship between the target genes by the "STRING" (https://string-db.org) (Confidence = 0.4). Subsequently, the network nodes were analyzed employing five algorithms, such as maximum clique centrality (MCC), Closeness, maximum neighborhood component (MNC), Degree, and edge percolated component (EPC). The biomarkers were identified by intersecting the top 10 genes of each algorithm. Furthermore, the expression levels of these biomarkers were examined in both the GSE125285 and GSE42109 datasets. Moreover, the receiver operating characteristic (ROC) curves of each biomarker in both the GSE125285 and GSE42109 datasets were used to assess the diagnostic values of the biomarkers. Based on this information, the nomogram was constructed to diagnose the risk of BCC utilizing the "RMS" R package (https://github.com/harrelfe/rms). Additionally, the validity of the diagnostic model was assessed using the calibration curve analysis.

### *The Gene Set Enrichment Analysis (GSEA) of Biomarkers*

The correlation coefficients between each biomarker and the target genes within the GSE125285 dataset were evaluated, and GSEA was performed to explore the underlying pathways of these biomarkers employing "clusterprofiler" R package (version 3.14.3, Bioconductor, Guangzhou, China) (adj.$p$.value $< 0.05$) [12].

## Results

### *A Total of 18 Target Genes were Associated with Transmembrane Transport and Phagocytosis*

There were 7314 DEGs (4958 up-regulated and 2356 down-regulated) between 25 BCC and 25 HC samples (Fig. 1A,B). The clustering analysis showed that there was no outlier sample (Fig. 2A). As shown in Fig. 2B, the optimal soft threshold value was identified as 15 and the Mean Connectivity was found close to 0. These findings indicated that the network approximated the scale-free distribution. Thus, a total of 14 modules were obtained based on the hybrid dynamic tree-cutting algorithm with MEDissThres = 0.3 (Fig. 2C). Subsequently, we analyzed the correlations between modules and traits. As depicted in Fig. 2D, the lightgreen module ($|R| = 0.93$, $p$ = 1e-22) exhibited the highest significant correlation with BCC. Therefore, the lightgreen module was identified as the key module and 6052 module genes underwent further analysis. Finally, 18 target genes, including *ADGRB1*, *UCP2*, *SLC6A6*, *SLC16A2*, *DNASE1*, *WNK1*, *MBTPS1*, *DOCK3*, *CD47*, *ELMO2*, *DOCK4*, *ABCA1*, *ADAM10*, *P2RX7*, *DNASE2*, *TNFRSF1A*, *SLC2A1*, and *P2RY2* were identified by intersecting 7314 DEGs, 6052 module genes, and 71 EGs (Fig. 2E).

The identified 18 target genes were enriched to 594 Gene Ontology (GO) functions, including vascular process in the circulatory system, phagocytosis, organic anion transport, and many others. Importantly, all these functions were found to be related to transmembrane transport. Furthermore, the target genes were enriched to 6 Kyoto Encyclopedia of Genes and Genomes (KEGG) pathways, including adipocytokine, thyroid hormone signaling pathways, insulin resistance, T-cell leukemia virus 1 infection, lipid and atherosclerosis, and apoptosis. Among them, the adipocytokine signaling pathway exhibited significantly higher enrichment ($p < 0.01$, Fig. 3A,B).

### *Construction of the Diagnostic Model of BCC*

The PPI network was constructed using 15 nodes and 12 protein interaction relationship pairs (Fig. 4A). Subsequently, the networks of the top 10 genes were constructed using five algorithms, such as Closeness, Degree, EPC, MCC, and MNC (Fig. 4B). Moreover, five biomarkers, including *ADAM10*, *MBTPS1*, *P2RY2*, *SLC2A1*, and *UCP2* were identified for further analyses (Fig. 4C). The expres-

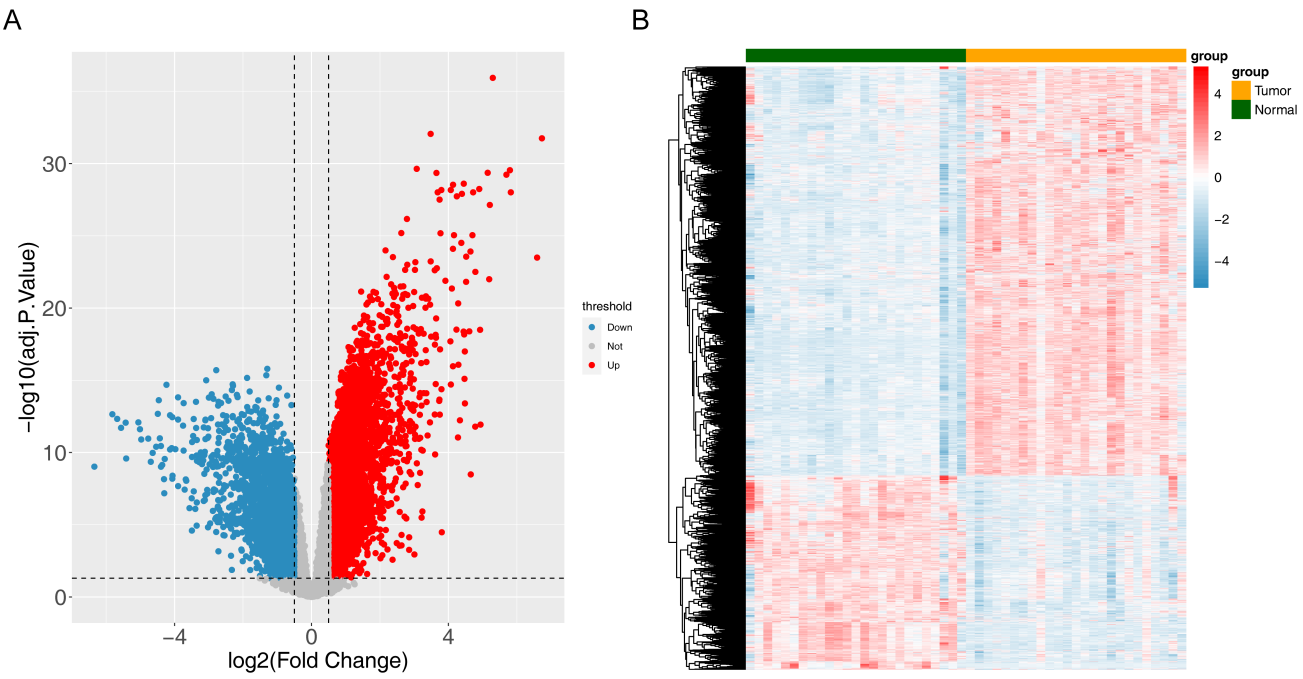


**Fig. 1. Identification of differentially expressed genes (DEGs) between basal cell carcinoma (BCC) and healthy control (HC) tissue samples.** (A) The volcano plot illustrates the distribution of DEGs based on statistical significance (x-axis) and fold change (y-axis). (B) The heatmap visualizes the expression levels of DEGs in BCC samples compared to the healthy control samples.

sion patterns of these biomarkers were consistent in both GSE125285 and GSE42109 datasets. Particularly, the expression levels of *MBTPS1* and *UCP2* were significantly higher, and *P2RY2* and *SLC2A1* were significantly lower in BCC samples (Fig. 5A,B). Furthermore, the area under the ROC curve (area under the curve (AUC) value) for each biomarker was higher than 0.8 in both GSE125285 and GSE42109 datasets, expect for *ADAM10* in GSE42109 (Fig. 5C,D). In the training set, *ADAM10* presented excellent performance in terms of diagnostic efficacy. In the validation set, the effect of *ADAM10* was resulting in a low AUC value. This could be due to factors such as differences between samples or batch effects. These findings supported the utilization of these five biomarkers for constructing the diagnostic model. Based on these findings, a nomogram was developed incorporating these five biomarkers. The calibration curve of the nomogram showed a close match between the disease risk prediction and the actual outcomes, indicating its potential as an effective diagnostic model (Fig. 5E,F).

### *Function Enrichment Analysis of Biomarkers*

The GSEA analysis results showed that the *ADAM10* was associated with the function of mitosis, *MBTPS1* and *P2RY2* were associated with immune response, *SLC2A1* was associated with ribonucleoprotein complex biogenesis, and *UCP2* was associated with positive regulation of cell migration. Interestingly, the functions of adaptive immune response and response to bacterium were negative with *MBTPS1* and positive with *P2RY2*. Additionally, *ADAM10* and *SLC2A1* showed an association with the nucleocytoplasmic transport pathway. Furthermore, *MBTPS1* showed a negative association, while *P2RY2* exhibited a positive association with the pathways involving cytokine-cytokine receptor interaction, hematopoietic cell lineage, and viral protein interaction with cytokine and cytokine receptors. Additionally, *SLC2A1* indicated a negative association, while *UCP2* showed a positive association with the EMC receptor interaction pathway (Fig. 6A–E).

## Discussion

Efferocytosis has been linked to cancer progression [15]. The effects of efferocytosis include recognition of dying cells, their phagocytosis, and homeostatic resolution. However, the specific impact of Efferocytosis-Related Genes (ERGs) in basal cell carcinoma (BCC) remains unclear. To the best of our knowledge, this is an inaugural investigation to delve into the potential role of ERGs in the context of BCC, aiming to shed light on unexplored aspects of cancer research.

In this study, we identified 18 genes associated with transmembrane transport and phagocytosis. Up to now, previous research has demonstrated that elevated SLC6A6 expression drives tumorigenesis [16]. Cancer immunotherapy relies on adaptive immune checkpoints such as PD-1. UV-damaged BCC usually manifests as tumors with a high tumor mutational burden (TMB), which can be significantly reduced by anti-PD-1 antibody therapy. The efficacy

Journal of
BIOLOGICAL REGULATORS
and Homeostatic Agents

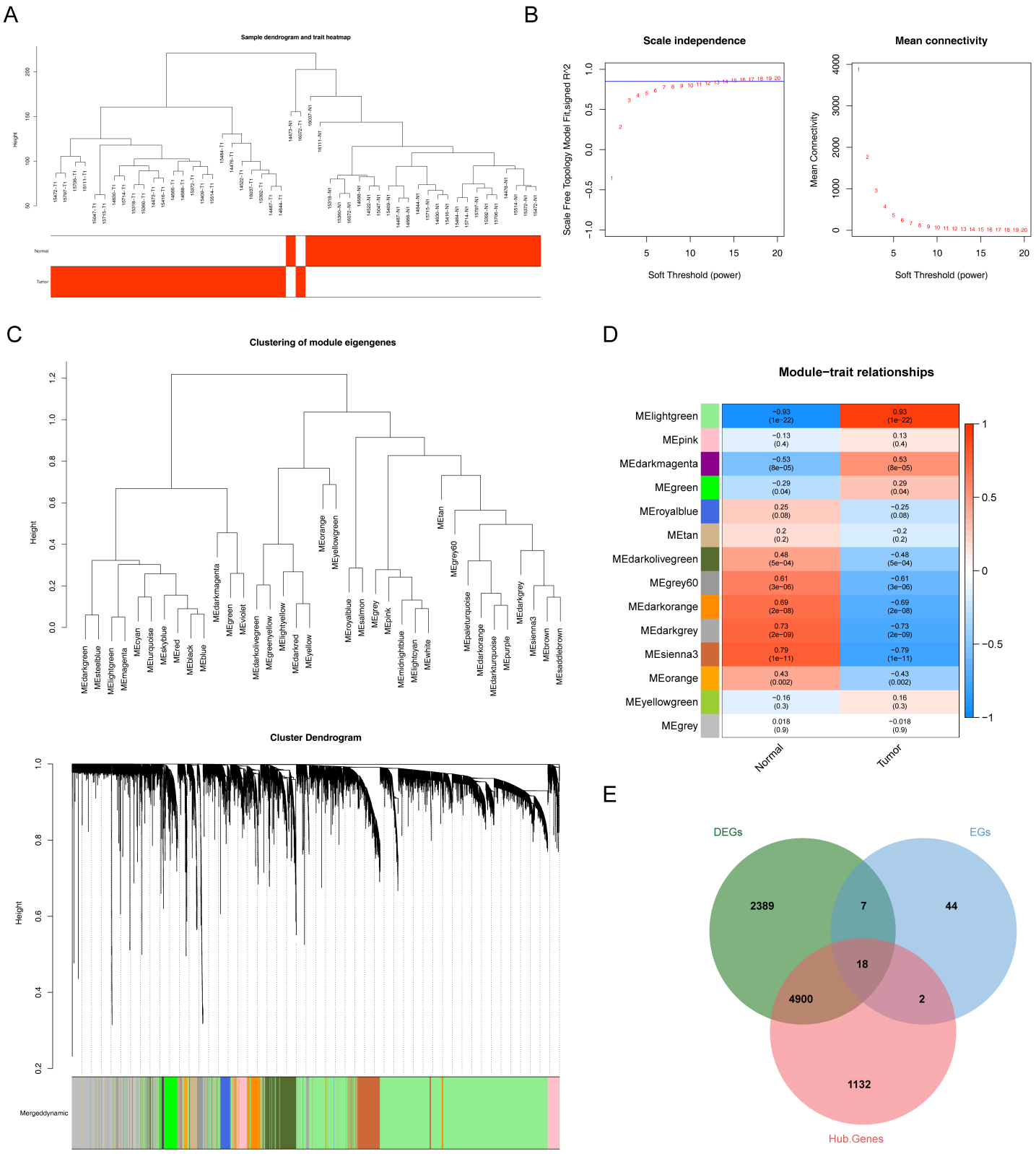


**Fig. 2. Identification of module genes of BCC by weighted gene co-expression network analysis (WGCNA).** (A) The clustering dendrogram and trait heatmap display the sample clustering based on gene expression profiles. (B) Analysis of the scale-free index helps determine the appropriate soft-threshold power for WGCNA. (C) The clustering of module eigengenes and cluster dendrogram, along with assigned module colors, show the co-expression patterns of genes. (D) Heatmap depicts the correlation between module eigengenes and normal/tumor status. (E) The Venn diagram illustrates the overlap of 18 target genes obtained from DEGs, module genes in WGCNA, and efferocytosis-related genes (EGs).

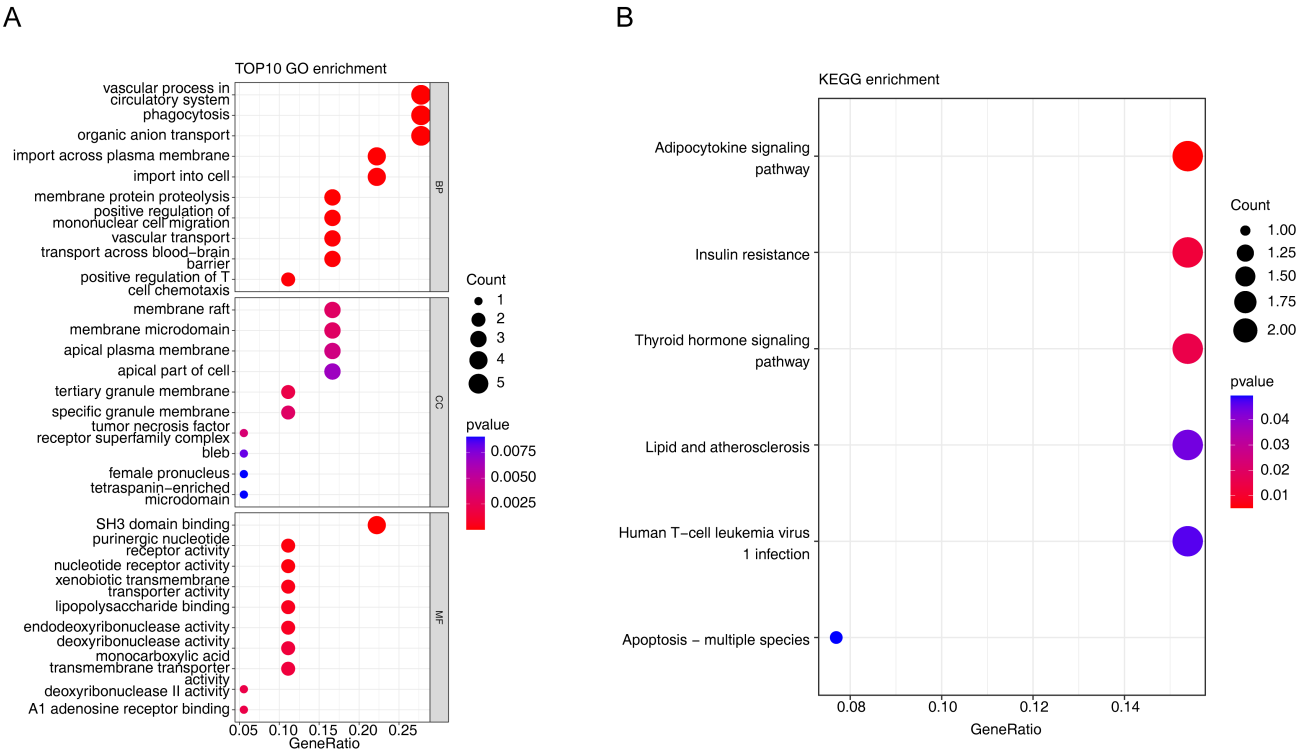


**Fig. 3. Functional enrichment analysis.** (A) Gene Ontology (GO) functions and (B) Kyoto Encyclopedia of Genes and Genomes (KEGG) pathways enrichment in target genes.

of PD-1 blockade antibodies in treating tumors depends on CD8 T cell function. A positive correlation has been observed between SLC6A6 expression and the effector T cell signature in CD8 T cells. Moreover, the knockdown of SLC6A6 in CD8 T cells has been shown to alter calcium signaling pathways, oxidative phosphorylation, and T cell receptor signaling [17]. Significantly, when treating BCC, the taurine transporter SLC6A6 selectively absorbs 5-ALA in the cells of the skin tumor [18]. SLC6A6 is involved in the absorption of aminolevulinic acid (ALA) and promotes the accumulation of protoporphyrin in cancer cells induced by ALA. Cells expressing SLC6A6 experienced more photodamage following ALA treatment [19]. Additionally, changes in the expression and function of the SLC6 family of soluble carrier proteins might be associated with cancer [20]. Recent research has reported the significant role of with-no-lysine kinase 1 (WNK1) in the proliferation and metastasis of tumor cells. BCC is a locally invasive malignant epidermal skin neoplasm, and WNK1 is one of the crucial genes uniquely associated with invasive cancers. Tumor-induced angiogenesis and proliferation of tumor cells are facilitated by interconnected signaling pathways [21], which regulate ion cotransporters and control cell responses to osmotic stress [22]. Through the WNK-OSR1/SPAK-NKCC cascade, with-no-lysine kinases (WNKs) contribute to ion homeostasis. The primary mechanism through which CD147 influences the properties of cancer subpopulations of tumor cells that display chemoresistance probably stems from its close relation to the processes driving malignancy, invasiveness, and potent tumorigenicity. It is currently thought that within the tumor microenvironment, CD147 promotes tumor proliferation while inhibiting cancer cell apoptosis. Moreover, CD147 influences tumor cell movement and metastasis through direct interactions with Annexin A2, the DOCK3-$\beta$-catenin-WAVE2 signaling axis [23]. Innate immunological checkpoints, such as SIRP$\alpha$ (signal-regulatory protein $\alpha$)/CD47, enable cancer cells to avoid immune monitoring. When CD47 binds to the SIRP$\alpha$ ligand on phagocytes, it enables cancer cells to escape the immune system [24]. In basal cell carcinoma, a strong correlation has been found between high CD47 expression and ulceration, as well as enhanced invasion [25]. Furthermore, the expression of the ATP-gated calcium channel $P2X_7$ increases the proliferation and invasion of cancer cells. The antibodies against the variant of $P2X_7$ (termed $nfP2X_7$) ointment are well-tolerated as a therapeutic for BCC [26]. Adhesion GPCR (aGPCR) ADGRB1 and its associated members have been implicated in different processes such as phagocytosis, leucocyte activation, and migration [27]. Hence, we speculated that *SLC6A6*, *WNK1*, *CD147*, and *CD47* were the core genes involved in transmembrane transport, while *ADGRB1* was the core gene of phagocytosis.

Five distinct biomarkers (*ADAM10*, *MBTPS1*, *P2RY2*, *SLC2A1*, and *UCP2*) were meticulously identified, leading to the construction of a robust diagnostic model. How-

Journal of
BIOLOGICAL REGULATORS
and Homeostatic Agents

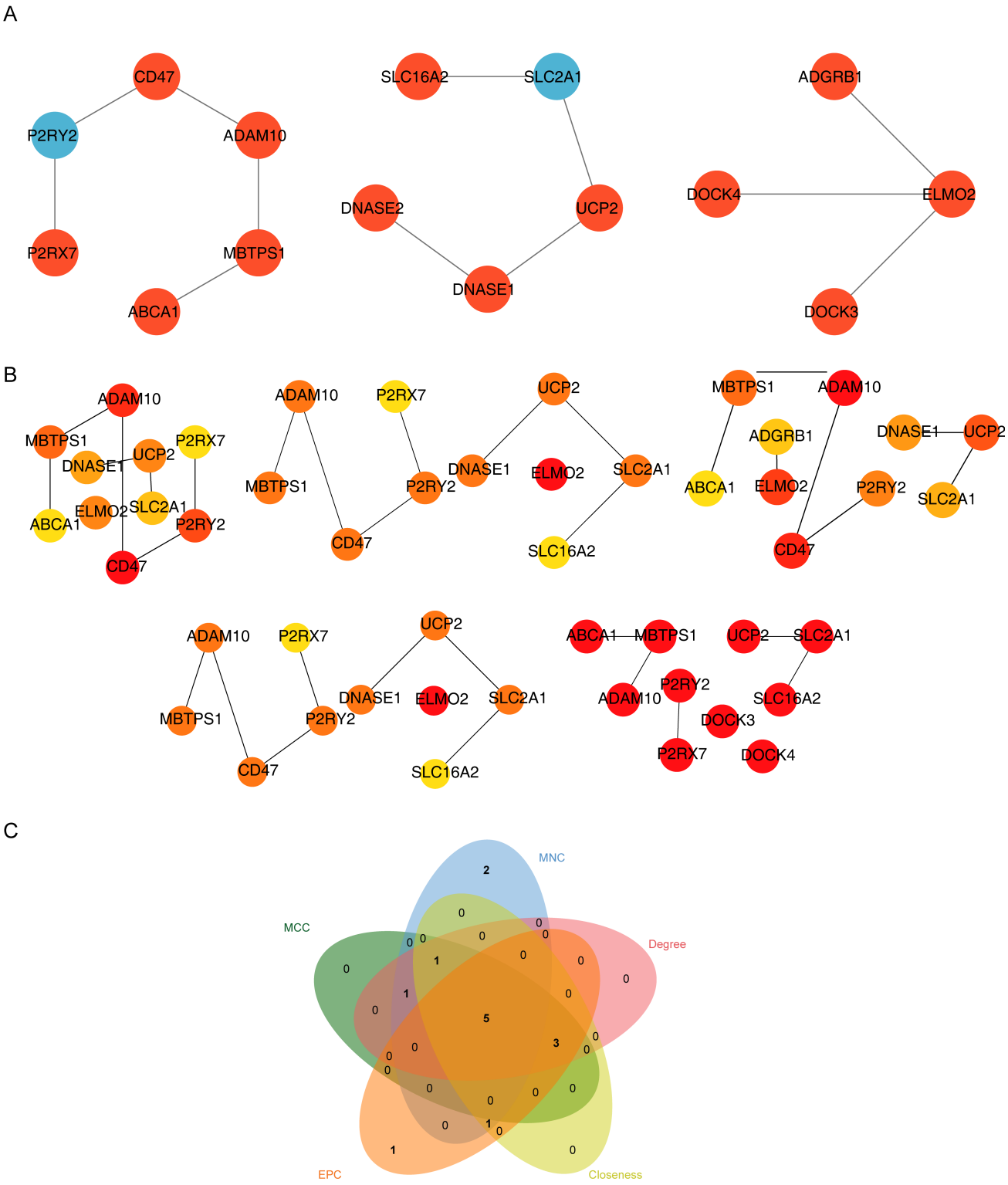


**Fig. 4. Identification of biomarkers for BCC.** (A) The protein-protein interaction (PPI) network of targets. (B) The networks of the top 10 genes were obtained using algorithms such as Closeness, Degree, EPC, MCC, and MNC. (C) The Venn diagram of five biomarkers was obtained by overlapping the top 10 genes in five algorithms. EPC, edge percolated component; MCC, maximum clique centrality; MNC, maximum neighborhood component.

ever, previous literature has underscored the pivotal role of cell communication and subsequent defensive responses in shaping immune reactions. Particularly, in this study, the associations of *MBTPS1* and *P2RY2* with adaptive immune responses shed light on their potential significance in the context of immunity modulation. Furthermore, our find-

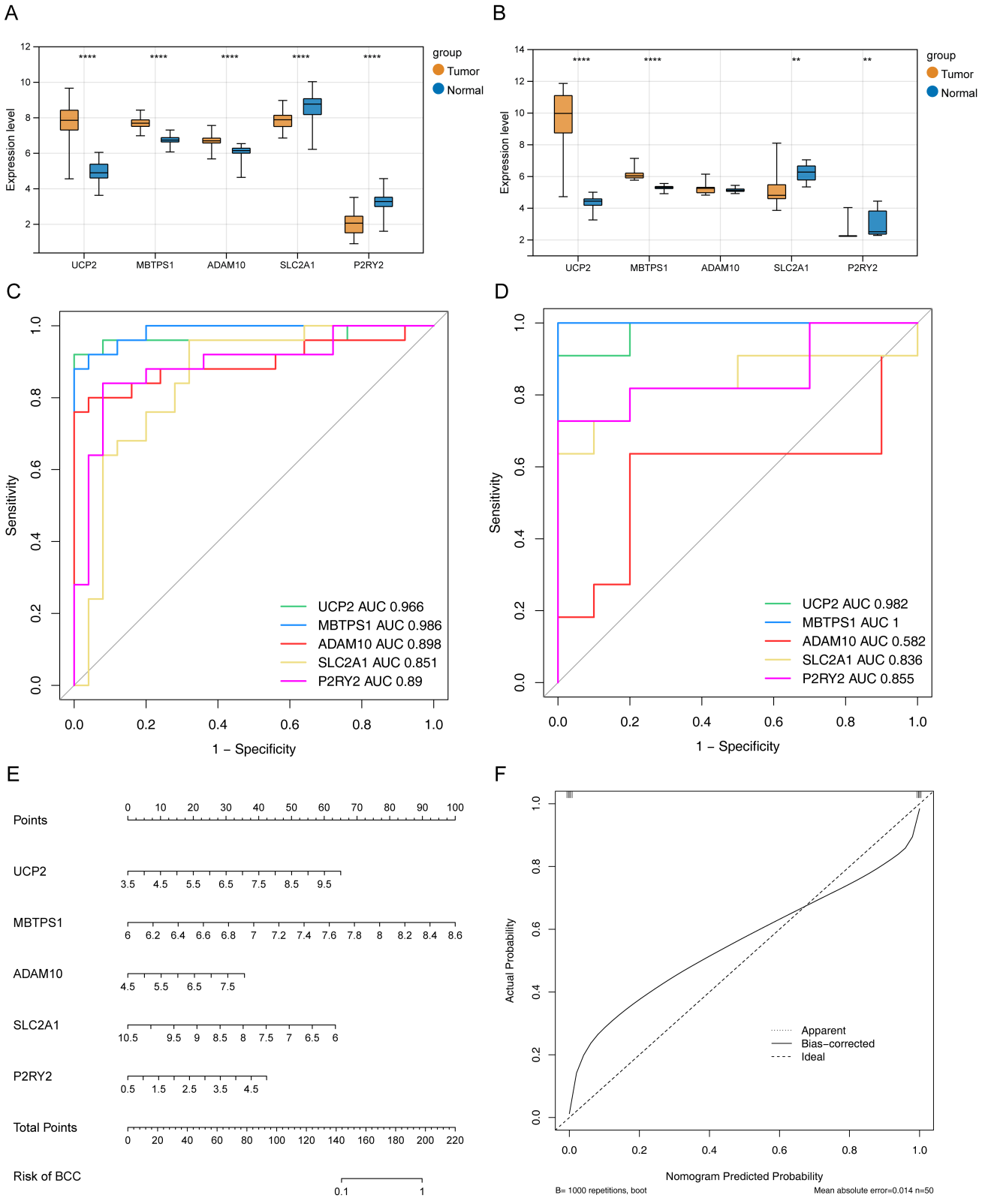


**Fig. 5. Analysis of five biomarkers.** (A,B) The expression patterns of five biomarkers in GSE125285 (A) and GSE42109 (B) datasets. (C,D) The receiver operating characteristic (ROC) curves of five biomarkers in both GSE125285 (C) and GSE42109 (D) cohorts. (E) The construction of nomogram to predict the risk of BCC. (F) The calibration curve of the nomogram. AUC, area under the curve. $^{**}p < 0.01$, $^{****}p < 0.0001$.

Journal of
BIOLOGICAL REGULATORS
and Homeostatic Agents

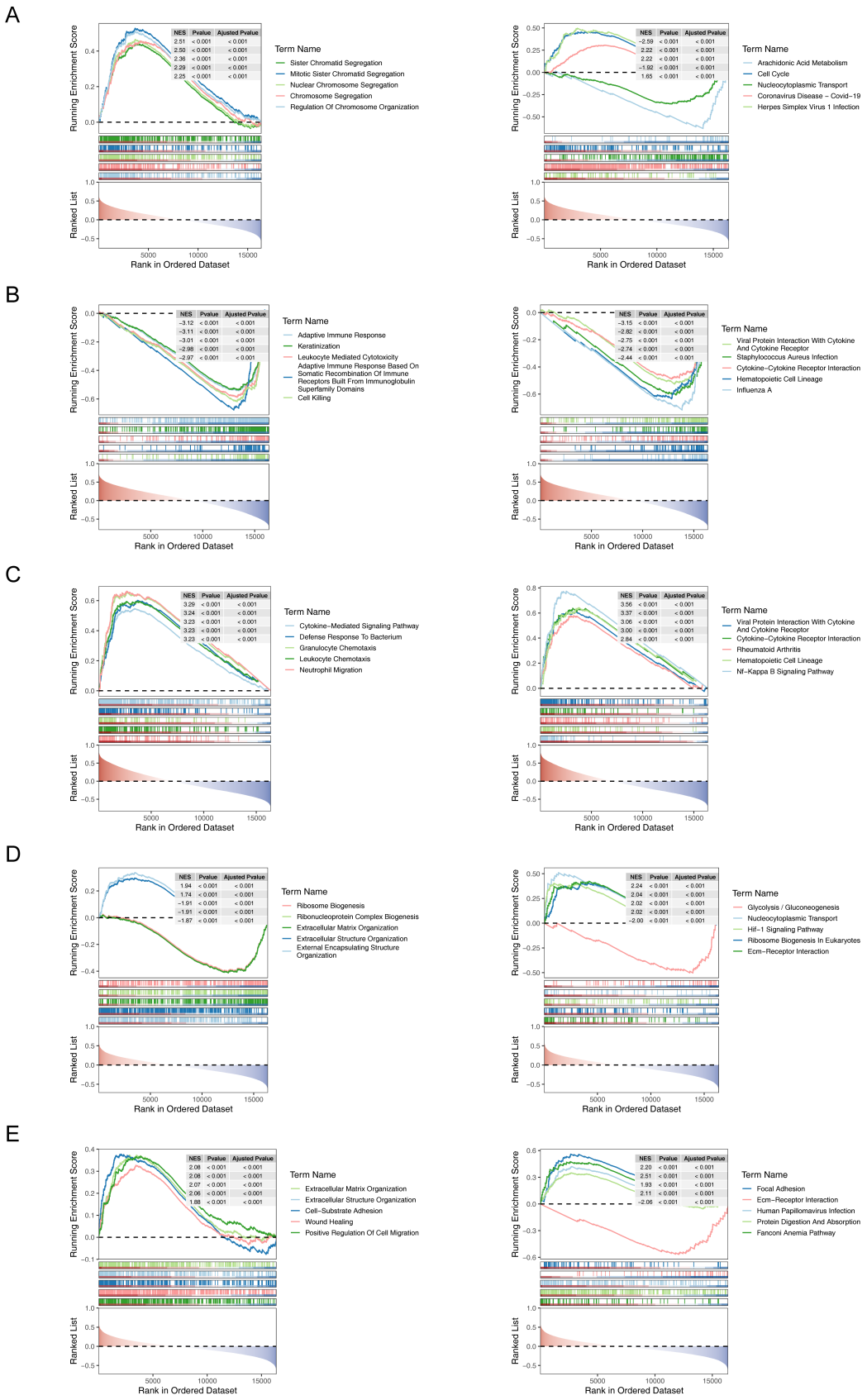


**Fig. 6. Gene set enrichment analysis (GSEA) of biomarkers.** (A–E) GO terms and KEGG pathways demonstrated enrichment in *ADAM10* (A), *MBTPS1* (B), *P2RY2* (C), *SLC2A1* (D), and *UCP2* (E).

ings align with previous study in demonstrating the overexpression of *ADAM10* immunoreactivity in deep invasion areas, suggesting the crucial involvement of this protease in the invasive, highly detrimental, and localized proliferation of BCC [28]. This correlation highlights the potential application of *ADAM10* as a key indicator of invasiveness and aggressiveness during BCC, thereby offering valuable insights into the underlying mechanisms driving the progression of this cancer. Sterol-regulatory element-binding proteins are involved in regulating cholesterol and fatty acid synthesis, which are two metabolic pathways implicated in cancer cell proliferation. *MBTPS1* cleaves sterol regulatory element-binding proteins to activate them [29]. The tumor microenvironment contains extracellular nucleotides that act as signaling elements. The research has suggested that extracellular nucleotides secreted by tumor cells and mediated by the *P2RY2* receptor may serve as regulators of invasiveness [30]. The function of *UCP2* is increased in many types of cancer and differs among cancer cells. Hep3B and HepG2 cells derived from hepatocellular carcinomas, as well as HT-29 cells from colorectal cancers, were treated with 5-azacytidine, revealing that Hep3B cells exhibited multiple methylated regions on the *UCP2* promoter [31]. *UCP2* levels correlate with tumor grade. High-proliferative neoplastic cells regulate *UCP2* to protect themselves against reactive oxygen species during chronic exposure [32]. *SLC2A1* mediates glucose uptake and promotes glycolysis. Cancer glycometabolism is governed by *SLC2A1*, which is widely expressed in cancers such as colorectal and pancreatic cancers [33]. Based on mechanistic studies of pancreatic cancer, forkhead box D1 induces transcription of *SLC2A1* and inhibits its degradation through RNA-induced silencing. Consequently, the expression of glucose transporter-1 (GLUT1) is enhanced, thereby regulating aerobic glycolysis to facilitate pancreatic cancer proliferation, invasion, and metastasis [34]. Colorectal cancer exhibiting high levels of *SLC2A1* shows elevated immune infiltration, m6A modification, and ferroptosis, as well as a distinct correlation between *SLC2A1* levels and cancer stage [35]. These findings indicate that these biomarkers exert their role through tumor invasion and affect the immune function, thereby impacting tumor development of BCC. These biomarkers have the potential for the development of a diagnostic model for BCC, warranting further investigation. Although our study demonstrated the potential importance of these five biomarkers in BCC and constructed a reliable diagnostic model, there are some limitations, mainly the lack of experimental validation. Specifically, our study primarily relied on bioinformatics analysis and literature review, lacking laboratory experiments to validate the function and mechanism of action of these biomarkers in basal cell carcinoma. Although bioinformatics analysis provided preliminary evidence to support our findings, further experimental studies are needed to validate the exact role of these biomarkers in disease progression.

## Conclusions

This study suggested a total of 18 target genes associated with transmembrane transport and phagocytosis, along with five efferocytosis-related biomarkers, offering promising diagnostic indicators for BCC. Furthermore, we suggest a new diagnostic model for BCC. These findings provide potential targets for clinical diagnosis and offer deeper insight into the regulatory mechanism of EGs in BCC.

## Availability of Data and Materials

The basal cell carcinoma related datasets GSE125285 and GSE42109 were downloaded from the Gene Expression Omnibus database (https://www.ncbi.nlm.nih.gov/geo/).

## Author Contributions

QCZ and WW designed the research study and performed the research. QCZ collected and analyzed the data. QCZ and WW have been involved in drafting the manuscript. Both authors have been involved in revising it critically for important intellectual content. Both authors gave final approval of the version to be published. Both authors have participated sufficiently in the work to take public responsibility for appropriate portions of the content and agreed to be accountable for all aspects of the work in ensuring that questions related to its accuracy or integrity.

## Ethics Approval and Consent to Participate

Not applicable.

## Acknowledgment

The authors would like to thank all the individuals and organizations that provided support for this study.

## Funding

This research received no external funding.

## Conflict of Interest

The authors declare no conflict of interest.

## References

[1] Basset-Seguin N, Herms F. Update in the Management of Basal Cell Carcinoma. Acta Dermato-venereologica. 2020; 100: adv00140.

[2] Gutzmer R, Solomon JA. Hedgehog Pathway Inhibition for the Treatment of Basal Cell Carcinoma. Targeted Oncology. 2019; 14: 253–267.

[3] Lin J, Xu A, Jin J, Zhang M, Lou J, Qian C, *et al*. MerTK-mediated efferocytosis promotes immune tolerance and tumor progression in osteosarcoma through enhancing M2 polarization and PD-L1 expression. Oncoimmunology. 2022; 11: 2024941.

Journal of
BIOLOGICAL REGULATORS
and Homeostatic Agents

[4] Perry JSA, Morioka S, Medina CB, Iker Etchegaray J, Barron B, Raymond MH, *et al*. Interpreting an apoptotic corpse as anti-inflammatory involves a chloride sensing pathway. Nature Cell Biology. 2019; 21: 1532–1543.
[5] Zhang Y, Wang Y, Ding J, Liu P. Efferocytosis in multisystem diseases (Review). Molecular Medicine Reports. 2022; 25: 13.
[6] Boada-Romero E, Martinez J, Heckmann BL, Green DR. The clearance of dead cells by efferocytosis. Nature Reviews. Molecular Cell Biology. 2020; 21: 398–414.
[7] Cheng Z, Wang L, Wu C, Huang L, Ruan Y, Xue W. Tumor-derived Exosomes Induced M2 Macrophage Polarization and Promoted the Metastasis of Osteosarcoma Cells Through Tim-3. Archives of Medical Research. 2021; 52: 200–210.
[8] Nguyen KQN, Tsou WI, Calarese DA, Kimani SG, Singh S, Hsieh S, *et al*. Overexpression of MERTK receptor tyrosine kinase in epithelial cancer cells drives efferocytosis in a gain-of-function capacity. The Journal of Biological Chemistry. 2014; 289: 25737–25749.
[9] Zhou Y, Yao Y, Deng Y, Shao A. Regulation of efferocytosis as a novel cancer therapy. Cell Communication and Signaling: CCS. 2020; 18: 71.
[10] Mehrotra P, Ravichandran KS. Drugging the efferocytosis process: concepts and opportunities. Nature Reviews. Drug Discovery. 2022; 21: 601–620.
[11] Trzeciak A, Wang YT, Perry JSA. First we eat, then we do everything else: The dynamic metabolic regulation of efferocytosis. Cell Metabolism. 2021; 33: 2126–2141.
[12] Colaprico A, Silva TC, Olsen C, Garofano L, Cava C, Garolini D, *et al*. TCGAbiolinks: an R/Bioconductor package for integrative analysis of TCGA data. Nucleic Acids Research. 2016; 44: e71.
[13] Langfelder P, Horvath S. WGCNA: an R package for weighted correlation network analysis. BMC Bioinformatics. 2008; 9: 559.
[14] Wu T, Hu E, Xu S, Chen M, Guo P, Dai Z, *et al*. clusterProfiler 4.0: A universal enrichment tool for interpreting omics data. Innovation (Cambridge (Mass.)). 2021; 2: 100141.
[15] Tajbakhsh A, Gheibi Hayat SM, Movahedpour A, Savardashtaki A, Loveless R, Barreto GE, *et al*. The complex roles of efferocytosis in cancer development, metastasis, and treatment. Biomedicine & Pharmacotherapy = Biomedecine & Pharmacotherapie. 2021; 140: 111776.
[16] Dazhi W, Jing D, Chunling R, Mi Z, Zhixuan X. Elevated SLC6A6 expression drives tumorigenesis and affects clinical outcomes in gastric cancer. Biomarkers in Medicine. 2019; 13: 95–104.
[17] Ping Y, Shan J, Liu Y, Liu F, Wang L, Liu Z, *et al*. Taurine enhances the antitumor efficacy of PD-1 antibody by boosting $CD8^+$ T cell function. Cancer Immunology, Immunotherapy: CII. 2023; 72: 1015–1027.
[18] Schary N, Novak B, Kämper L, Yousf A, Lübbert H. Identification and pharmacological modification of resistance mechanisms to protoporphyrin-mediated photodynamic therapy in human cutaneous squamous cell carcinoma cell lines. Photodiagnosis and Photodynamic Therapy. 2022; 39: 103004.
[19] Tran TT, Mu A, Adachi Y, Adachi Y, Taketani S. Neurotransmitter transporter family including SLC6A6 and SLC6A13 contributes to the 5-aminolevulinic acid (ALA)-induced accumulation of protoporphyrin IX and photodamage, through uptake of ALA by cancerous cells. Photochemistry and Photobiology. 2014; 90: 1136–1143.
[20] Stary D, Bajda M. Taurine and Creatine Transporters as Potential Drug Targets in Cancer Therapy. International Journal of Molecular Sciences. 2023; 24: 3788.
[21] Hou CY, Ma CY, Yuh CH. WNK1 kinase signaling in metastasis and angiogenesis. Cellular Signalling. 2022; 96: 110371.
[22] Jung JU, Jaykumar AB, Cobb MH. WNK1 in Malignant Behaviors: A Potential Target for Cancer? Frontiers in Cell and Developmental Biology. 2022; 10: 935318.
[23] Cui HY, Wang SJ, Miao JY, Fu ZG, Feng F, Wu J, *et al*. CD147 regulates cancer migration via direct interaction with Annexin A2 and DOCK3-$\beta$-catenin-WAVE2 signaling. Oncotarget. 2016; 7: 5613–5629.
[24] Jia X, Yan B, Tian X, Liu Q, Jin J, Shi J, *et al*. CD47/SIRP$\alpha$ pathway mediates cancer immune escape and immunotherapy. International Journal of Biological Sciences. 2021; 17: 3281–3287.
[25] Bang S, Jee S, Son H, Cha H, Park H, Myung J, *et al*. CD47 Expression in Non-Melanoma Skin Cancers and Its Clinicopathological Implications. Diagnostics (Basel, Switzerland). 2022; 12: 1859.
[26] Gilbert SM, Gidley Baird A, Glazer S, Barden JA, Glazer A, Teh LC, *et al*. A phase I clinical trial demonstrates that nfP2X_7 -targeted antibodies provide a novel, safe and tolerable topical therapy for basal cell carcinoma. The British Journal of Dermatology. 2017; 177: 117–124.
[27] Nijmeijer S, Vischer HF, Leurs R. Adhesion GPCRs in immunology. Biochemical Pharmacology. 2016; 114: 88–102.
[28] Oh ST, Schramme A, Stark A, Tilgen W, Gutwein P, Reichrath J. The disintegrin-metalloproteinases ADAM 10, 12 and 17 are upregulated in invading peripheral tumor cells of basal cell carcinomas. Journal of Cutaneous Pathology. 2009; 36: 395–401.
[29] Hartal-Benishay LH, Saadi E, Toubiana S, Shaked L, Lalzar M, Abu Hatoum O, *et al*. MBTPS1 regulates proliferation of colorectal cancer primarily through its action on sterol regulatory element-binding proteins. Frontiers in Oncology. 2022; 12: 1004014.
[30] Martínez-Ramírez AS, Garay E, García-Carrancá A, Vázquez-Cuevas FG. The P2RY2 Receptor Induces Carcinoma Cell Migration and EMT Through Cross-Talk with Epidermal Growth Factor Receptor. Journal of Cellular Biochemistry. 2016; 117: 1016–1026.
[31] Kim DY, Cheong HT, Ra CS, Kimura K, Jung BD. Effect of 5-azacytidine (5-aza) on UCP2 expression in human liver and colon cancer cells. International Journal of Medical Sciences. 2021; 18: 2176–2186.
[32] Vallejo FA, Vanni S, Graham RM. UCP2 as a Potential Biomarker for Adjunctive Metabolic Therapies in Tumor Management. Frontiers in Oncology. 2021; 11: 640720.
[33] Zheng H, Long G, Zheng Y, Yang X, Cai W, He S, *et al*. Glycolysis-Related SLC2A1 Is a Potential Pan-Cancer Biomarker for Prognosis and Immunotherapy. Cancers. 2022; 14: 5344.
[34] Cai K, Chen S, Zhu C, Li L, Yu C, He Z, *et al*. FOXD1 facilitates pancreatic cancer cell proliferation, invasion, and metastasis by regulating GLUT1-mediated aerobic glycolysis. Cell Death & Disease. 2022; 13: 765.
[35] Liu XS, Yang JW, Zeng J, Chen XQ, Gao Y, Kui XY, *et al*. SLC2A1 is a Diagnostic Biomarker Involved in Immune Infiltration of Colorectal Cancer and Associated With m6A Modification and ceRNA. Frontiers in Cell and Developmental Biology. 2022; 10: 853596.